

Assessment of chemotherapy response in non-Hodgkin lymphoma involving the neck utilizing diffusion kurtosis imaging: a preliminary study

Rui Wu*
Shi-Teng Suo*
Lian-Ming Wu
Qiu-Ying Yao
Hong-Xia Gong
Jian-Rong Xu

PURPOSE

We aimed to examine the utility of non-Gaussian diffusion kurtosis imaging (DKI) for assessment of chemotherapy response in patients with cervical (neck) non-Hodgkin lymphoma (NHL).

METHODS

Patients with cervical NHL underwent 3.0 T magnetic resonance imaging with maximal b value of 2000 s/mm² at baseline and seven days after chemotherapy onset. Apparent diffusion coefficient (ADC) value and diffusion kurtosis imaging maps for diffusion coefficient (*D*) and kurtosis (*K*) were calculated. Based on clinical examination, laboratory screening, and PET/CTs, patients were classified as responders or nonresponders.

RESULTS

Twenty-six patients were enrolled. Among them, 24 patients were classified as responders and two as nonresponders. For responders, mean follow-up ADC and *D* increased significantly compared with baseline (ADC: $0.92 \pm 0.11 \times 10^{-3}$ mm²/s vs. $0.68 \pm 0.11 \times 10^{-3}$ mm²/s; *D*: $1.47 \pm 0.32 \times 10^{-3}$ mm²/s vs. $0.98 \pm 0.21 \times 10^{-3}$ mm²/s, $P < 0.001$ for both). Mean follow-up *K* decreased significantly compared with baseline (1.14 ± 0.10 vs. 1.47 ± 0.19 , $P < 0.001$) for responders. D_{ratio} showed significant positive correlation and high agreement with ADC_{ratio} ($r = 0.776$, $P < 0.001$). Likewise, K_{ratio} showed significant negative correlation and high agreement with ADC_{ratio} ($r = -0.658$, $P < 0.001$).

CONCLUSION

The new DKI model may serve as a new biomarker for the evaluation of early chemotherapy response in NHL.

Non-Hodgkin lymphoma (NHL) is one of the most common types of lymphoma with an estimated 69 740 new cases and 19 020 deaths projected to occur in the United States in 2013 (1). First line treatment of NHL is usually chemotherapy, as it is known to be chemotherapy-sensitive. In lymphoma patients, the therapeutic options and grading depend on the histology of lymphoma, clinical stage, manifestation, and early response to treatment, in which follow-up imaging plays a major role (2, 3).

In order to diagnose, stage, and assess treatment response, contrast-enhanced computed tomography (CT) has been the most widely used technique. Recently, utilization of [18F] Fluorodeoxyglucose (FDG)-positron emission tomography (PET) alone or combined with CT (PET/CT) has been increasing due to its greater sensitivity in detecting active disease (4–6). Although it has been reported that interim PET during treatment will forecast the outcome in patients with diffuse large B-cell lymphoma, the clinical utility of FDG-PET for assessing the early treatment response has not been confirmed (7–9).

Diffusion-weighted imaging (DWI) provides detailed anatomic and functional information and has documented value in the diagnosis, staging, and treatment monitoring of lymphoma (10, 11). The quantitative parameter of DWI, apparent diffusion coefficient (ADC) acquired from Gaussian model, reflects tissue cellularity, extracellular water content and organization. DWI, which is a functional magnetic resonance imaging (MRI) technique, has been demonstrated to be particularly valuable in assessing the treatment response of lymphoma (12–14).

However, due to various barriers, such as cellular membranes and compartments, water diffusion behavior follows a non-Gaussian model. As an advanced DWI model, diffusion kurtosis imaging (DKI) quantifies non-Gaussian distribution of water diffusion behavior and

From the Department of Radiology (H.X.G., ✉ ghx_rj@163.com, J.R.X. ✉ xujiannr@yeah.net) Renji Hospital, Shanghai Jiao Tong University School of Medicine, Shanghai, China.

*These authors contributed equally to this work.

Received 14 April 2016; revision requested 24 June 2016; last revision received 31 October 2016; accepted 3 November 2016.

Published online 5 April 2017.
DOI 10.5152/dir.2017.16184

provides not only a corrected ADC, but also the excess kurtosis of tissue (15). It is considered that this new imaging analysis method is more sensitive to reflect the complexity of tissue microstructure than the conventional monoexponential model (16, 17). DKI has been demonstrated to be of great value when estimating the grading of many diseases, such as brain disorders (18, 19), head and neck cancers (20), bladder cancers (21), prostate cancer (22), hepatocellular carcinoma (23), and breast lesions (24). Considering the microstructure of lymphoma, it is proposed that the non-Gaussian model could be a better predictor for the chemotherapy response in lesions. As far as we know, no data are available regarding the diagnostic value of DKI-derived ADC, corrected diffusion coefficient (D) and kurtosis (K) for examining the response to chemotherapy in lymphoma patients. Hence, the aim of this study is to examine the utility of DKI for assessment of chemotherapy response in non-Hodgkin lymphoma patients.

Methods

Patients

This study was approved by the local institutional review board, and all patients gave written informed consent before the study. Patients with histologically proven cervical non-Hodgkin lymphoma scheduled to receive standard chemotherapy were enrolled. The exclusion criteria were history of previous non-lymphoma malignancy and/or hematologic disorders, contraindications to MRI (e.g., claustrophobia, implanted pacemakers), or not giving consent to the study.

3.0 T MRI examinations were obtained, which included routine sequences along with cine T2-weighted imaging and DKI, at baseline and seven days after chemotherapy onset. Patients underwent baseline MRI and started chemotherapy the next day.

Main points

- Diffusion kurtosis imaging can estimate the chemotherapy response in patients with cervical (neck) non-Hodgkin lymphoma (NHL).
- The amplitude of D was positively associated with the amplitude of ADC, while the amplitude of K showed an inverse correlation with ADC.
- The amplitude of D and K may be an alternative tool to ADC for determining the chemotherapy response in NHL patients.

MRI protocol

All subjects underwent a standard scan protocol using a 3.0T MRI scanner (HDxt; GE Healthcare). A phased-array 8-channel neck coil was used. An axial T1-weighted spin echo imaging was used for routine neck MRI. The parameters included repetition time (TR), 420 ms; echo time (TE), 7 ms; field of view (FOV), 220×220 mm; section thickness, 5 mm; intersection gap, 1 mm; matrix size, 320×152; number of excitation, 1. Subsequently, a free-breathing fat-suppressed single-shot echo-planner sequence was used for the DKI scan with b values of 0, 500, 700, 1200, 1500 and 2000 s/mm², along the three orthogonal axes of the magnet with the following parameters: TR, 5200 ms; TE, 68 ms; FOV, 280×280 mm; section thickness, 3 mm; intersection gap, 1 mm; matrix size, 132×128; number of excitation, 1. In order to achieve the best correlation of morphologic changes between CT and MRI modalities, b value of 0 s/mm² was used. Likewise, to ensure a large enough effect on the DWI signal, b value of 2000 s/mm² was used (23, 25).

Image analysis

Two radiologists, with four and 12 years of experience in MRI, blinded to patient's diagnosis (NHL subtype) and the kind of therapy, interpreted both routine MRI and DKI data in consensus. Region of interest (ROI) was placed over lymphoma localization on b=0 images, so as to remain inside the margins of the target lesion in order to ensure the accuracy of measurement.

Both MRI and DKI data were analyzed with Matlab (version R 2011 b; MathWorks). Voxel-by-voxel analysis was used in this program and the multi-b DKI signal intensities (S) were fitted. The following equation was used:

$$S = S_0 \times \exp(-b \times D + b^2 \times D^2 \times K/6)$$

In which b represents b value, D represents ADC corrected for non-Gaussian diffusion behavior and K represents excess kurtosis. Larger K manifests greater deviation from the conventional monoexponential model distribution. A conventional Gaussian distribution model was used to calculate the standard ADC. All b values were fitted and the following equation was used:

$$S = S_0 \times \exp(-b \times ADC)$$

The maps of ADC, D and K were outputted through the below calculations. The ADC, D and K changes (ADC_{ratio} , D_{ratio} and K_{ratio} in %) for each patient at baseline

and seven days after treatment onset were calculated using the formula as follows: $ADC_{ratio} = (ADC_{post} - ADC_{baseline})/ADC_{baseline} \times 100\%$; then both D_{ratio} and K_{ratio} were calculated according this formula. Based on the clinical examination, laboratory screening and PET/CT, patients were classified as responders or nonresponders (26).

Statistical analysis

SPSS for windows (version 19.0; IBM Inc.) and MedCalc for window (version 11.4.0.0; MedCalc Software) were used to analyze the data. Shapiro-Wilk test and quantile-quantile plots were used to test the normality of the data. Normally distributed data are presented as mean \pm standard deviation. Differences at baseline and seven days after chemotherapy onset in ADC, D and K were compared using the paired sample t-test. Correlation between parameters was determined by Pearson correlation coefficient and agreement between parameters was examined by Bland-Altman test. A value of $P < 0.05$ was considered statistically significant.

Results

Between July 2013 and September 2015, 40 consecutive patients who met the inclusion criteria were included in this prospective study. Histologic biopsy was performed to confirm the subtype of lymphoma. Standard chemotherapy with RCHOP (rituximab, cyclophosphamide, vincristine, doxorubicin, and prednisone) was utilized for diffuse large B-cell lymphoma and T-cell lymphoma, and CHOP (all except rituximab) was utilized for follicular lymphoma. Six patients who needed radiotherapy during chemotherapy were excluded and six patients refused to undergo MRI examination after consenting for the study. In addition, two patients did not complete the treatment schedule due to treatment-induced toxicity and were also excluded. Consequently, a final cohort of 26 patients (14 male and 12 female patients; average age, 48.5 \pm 15.3 years) was included in the study. Histologic biopsy revealed the following subtypes: diffuse large B-cell lymphoma (n=20), T-cell lymphoma (n=2), and follicular lymphoma (n=4). There were 24 responders and two nonresponders.

The mean ADC and D values of the responders increased between baseline and follow-up study ($P < 0.001$, for both), while the mean K value decreased ($P < 0.001$) (Ta-

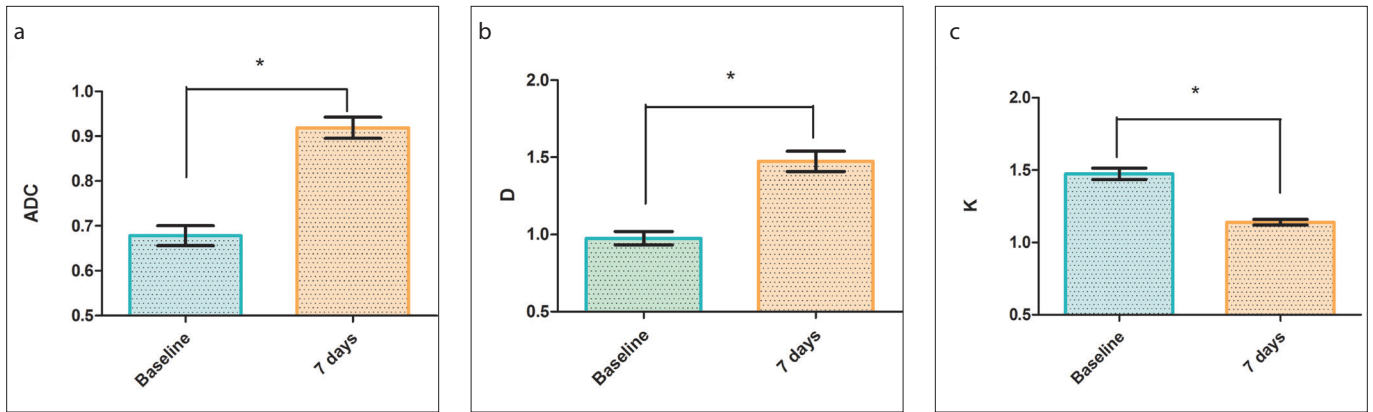


Figure 1. a–c. Boxplot of ADC (10^{-3} mm²/s) (a), D (10^{-3} mm²/s) (b) and K (c) (n=24). Error bars are mean \pm standard error of mean (SEM). * significant difference compared with baseline.

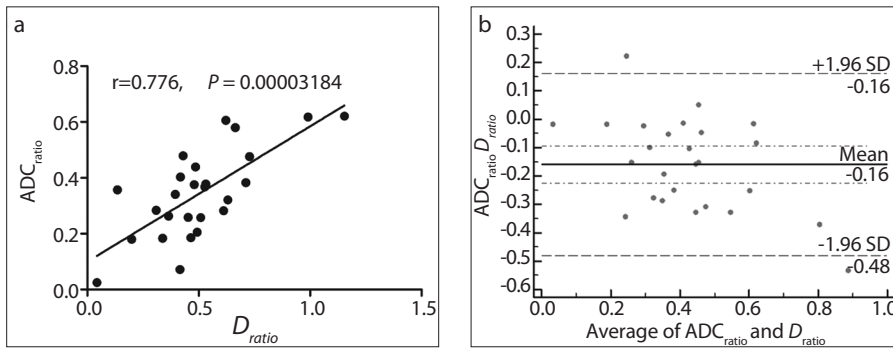


Figure 2. a, b. Scatter plots depict correlations between ADC_{ratio} and D_{ratio} . Significantly positive correlation is present between ADC_{ratio} and D_{ratio} (a, $r=0.776$, $P < 0.001$). Bland-Altman test (b) shows good agreement between ADC_{ratio} and D_{ratio} .

Parameters	Responders (n=24)		Nonresponders (n=2)	
	At baseline	7 days after chemotherapy onset	At baseline	7 days after chemotherapy onset
ADC ($\times 10^{-3}$ mm ² /s)	0.68 \pm 0.11	0.92 \pm 0.11*	0.76 \pm 0.31	0.79 \pm 0.33
D ($\times 10^{-3}$ mm ² /s)	0.98 \pm 0.21	1.47 \pm 0.32*	1.04 \pm 0.48	1.08 \pm 0.49
K	1.47 \pm 0.19	1.14 \pm 0.10**	1.30 \pm 0.34	1.30 \pm 0.34

*Increased significantly compared with baseline in responders, $P < 0.001$.
 **Decreased significantly compared with baseline in responders, $P < 0.001$.

Patients	ADC_{ratio} (%)	D_{ratio} (%)	K_{ratio} (%)
Responders (n=24)	36.9 \pm 13.8	52.7 \pm 22.4	-21.7 \pm 9.5
Nonresponders (n=2)	3.3 \pm 1.1	4.6 \pm 4.7	-0.4 \pm 0.3

ble 1, Figs. 1, 2). We assessed the change of amplitude between baseline and follow-up imagings (Table 2).

In addition, D_{ratio} showed significantly positive correlation and high agreement with ADC_{ratio} ($r=0.776$, $P < 0.001$) (Fig. 2). Likewise, K_{ratio} showed significantly negative correlation

and high agreement with ADC_{ratio} ($r = -0.658$, $P < 0.001$) (Fig. 3). Fig. 4 shows DKI findings of a patient with large B-cell lymphoma.

Discussion

As far as we know, this is the first study utilizing the DKI model to assess chemotherapy

response in patients with NHL. In this study, we successfully used the DKI model to examine the chemotherapy response for NHL and found that changes in the three main parameters (ADC, D and K) showed good correlation with the clinical responses. The value of ADC and D increased significantly after seven days of chemotherapy compared with baseline in treatment responder NHL patients. The value of K showed inverse trend to ADC and D . The amplitude of D change during treatment was positively correlated with ADC, whereas the amplitude of K change showed an inverse correlation with ADC. These parameters reflected the chemotherapy response in a non-Gaussian water diffusion pattern, which is inclined to offer greater sensitivity measuring the complexity of tissue microstructure.

Jensen et al. (15) first reported that the DKI model could better estimate brain tissue characterization because of its greater sensitivity than the conventional DWI in 2005. The DKI model, which is based on a non-Gaussian distribution assumption, is believed to show the true diffusion distribution characteristics of heterogeneous tissue microenvironment, in contrast to the Gaussian model, which is a conventional monoexponential model. The utility of kurtosis modeling for head and neck squamous cell carcinoma has been shown to be feasible and provided a better analysis than did monoexponential modeling (20). Suo et al. (21) applied the DKI model to assess the histologic grade of bladder cancer and concluded that the DKI model can reflect the diffusion of bladder cancer. In the meanwhile, K may be a new biomarker for grading of bladder cancer. In contrast to conventional diffusion imaging parameters, the DKI derived from non-Gaussian model can better separate high-grade gliomas and

primary central nervous system lymphomas (27). Therefore, the value of DKI model in estimating the stage and grade of different diseases is well established.

In our study, we found that in responders, the mean ADC and D increased significantly compared with baseline, and the mean K decreased significantly compared with baseline, which could reflect the chemotherapy response in NHL patients. In our cohort, the ADC values significantly increased by $36.9\% \pm 13.8\%$ on day 7 after chemotherapy onset for responders. Others have reported that ADC values in diffuse large B-cell lymphoma patients increased significantly after treatment and concluded that change of ADC might help to estimate the treatment response in lymphoma patients (28).

Recently, three studies investigated the change in ADC values during chemotherapy treatment of lymphoma. Horger et al. (12) combined ADC values and lesion sizes to estimate the feasibility for whole-body DWI to assess early chemotherapy response in lymphoma patients. Their study demonstrated that the mean ADC value increased for responders whereas lesion size decreased. Wu et al. (29) noted a significantly increased ADC value after one week and two cycles of chemotherapy, which correlated with PET/CT results, as well as the decrease in tumor volume. Paepe et al. (30) evaluated the change of ADC value at two and four weeks during treatment in NHL patients, and the amplitude of ADC at two and four weeks after complete remission and

reported that the amplitude of ADC may reflect the response to treatment.

Our current study shows the ability of D and K values to assess the chemotherapy response in NHL patients. Interestingly, we found that the amplitude of change in D values was the highest among three parameters. While numerous factors affect these parameters, it is more accurate to measure tissue diffusion with D value, which corrects the conventional Gaussian diffusion distribution. A possible fundamental reason for this is that DKI model based on non-Gaussian diffusion reflects both tissue diffusion and kurtosis behavior. Compared with ADC and K values, the contribution of diffusivity in D value estimation might be greater. Although it is also influenced by other extracellular factors, K value of tissues has been presumed to represent the direct interaction of water molecules with cell membranes and intracellular compounds (31, 32). Rosenkrantz et al. (23) used *ex vivo* evaluation of DKI model to assess hepatocellular carcinoma and presence of treatment-related necrosis, and found that D was greater than ADC. They concluded that the DKI model might potentially provide additional value as a biomarker in hepatocellular carcinoma characterization.

Significant relationships between ADC_{ratio} and D_{ratio} as well as between ADC_{ratio} and K_{ratio} in NHL patients were observed in our study. The D_{ratio} was positively correlated

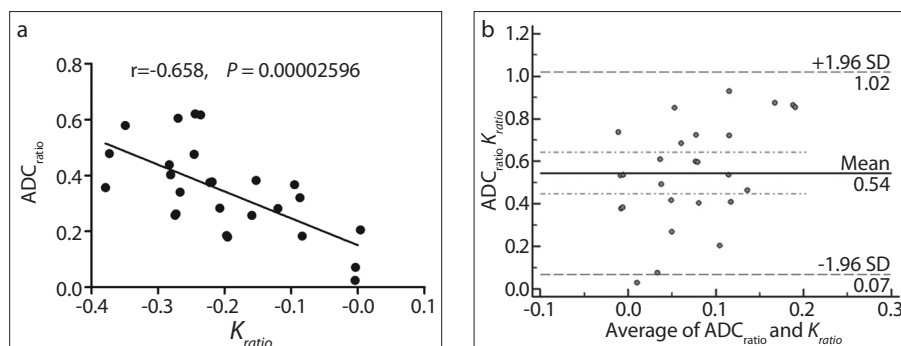


Figure 3. a, b. Scatter plots depict correlations between ADC_{ratio} and K_{ratio} . Significantly negative correlation is present between ADC_{ratio} and K_{ratio} (a, $r = -0.658$, $P < 0.001$). Bland-Altman test (b) shows good agreement of ADC_{ratio} and K_{ratio} .

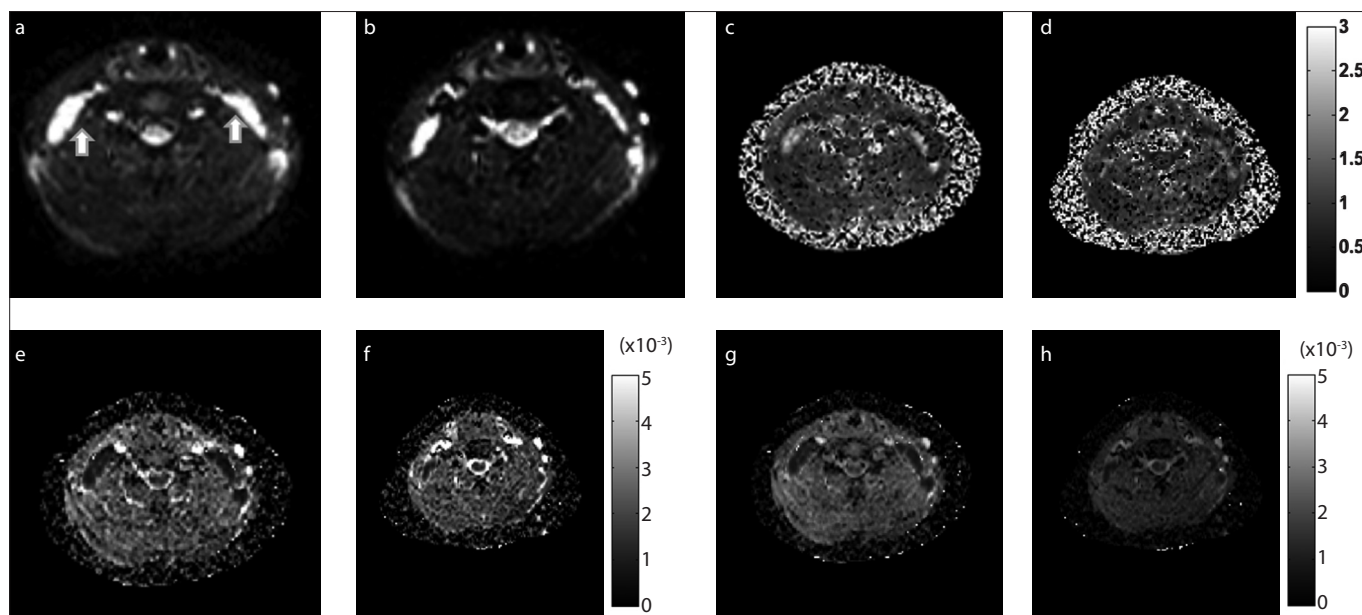


Figure 4. a–h. Images with $b=0$ of a 57-year-old man with diffuse large B-cell lymphoma diagnosed via histologic biopsy. Axial T2-weighted images show two lesions in the neck at baseline (a, arrows) and seven days after chemotherapy onset (b). The K maps (c, d) show that follow-up K values of lesions decrease compared with baseline (1.93 vs. 1.27). The D maps (e, f) show that follow-up D values of lesions increase compared with baseline ($0.62 \times 10^{-3} \text{ mm}^2/\text{s}$ vs. $1.34 \times 10^{-3} \text{ mm}^2/\text{s}$). The ADC maps (g, h) show that follow-up ADC values of lesions increase compared with baseline ($0.52 \times 10^{-3} \text{ mm}^2/\text{s}$ vs. $0.71 \times 10^{-3} \text{ mm}^2/\text{s}$).

with the ADC_{ratio} . Meanwhile, the K_{ratio} was negatively correlated with the ADC_{ratio} . Effective treatment for NHL patients reducing the cellularity and disordered vasculature and resulting in an increased amplitude of ADC and D values might account for these relationships. A similar study using the DKI model to estimate the histologic grade of bladder cancer demonstrated that ADC value was significantly higher in low-grade bladder cancer and lower in high-grade bladder cancer, while K value showed an inverse trend (21).

There were some limitations to our study. First, this was a single-center study with a small sample size. Although we showed that the use of a non-Gaussian diffusion model for assessing the chemotherapy response is feasible, much larger sample size and multiple center studies are needed to investigate the potential outlook of the DKI model to diagnose, stage, and grade NHL. Second, due to the small sample size, this study did not provide a cutoff value for the ratios of ADC, D , and K . Third, no analysis of lesion size or tumor volume was used to investigate the relationship between these three parameters. Horger et al. (12) reported 73% increase in ADC and 15.8% decrease in maximal lesion diameter, as cutoff values for responders at a median of seven days after treatment, based on the response at six months. The clinical utility of the DKI model has formerly been confirmed *in vivo* for head-and-neck carcinomas and gliomas. Our study was limited to lesions in the neck and lesions in other locations were not included. To the best of our knowledge, this is the first study using the DKI model to estimate the chemotherapy response in NHL patients. The feasibility of whole-body DKI for clinical use should be examined.

In conclusion, the use of DKI model for estimating the chemotherapy response in NHL patients is feasible and may serve as a new biomarker for evaluation of early chemotherapy response in NHL.

Conflict of interest disclosure

The authors declared no conflicts of interest.

References

- Siegel R, Naishadham D, Jemal A. Cancer statistics, 2013. *CA Cancer J Clin* 2013; 63:11–30. [\[CrossRef\]](#)
- Lin C, Luciani A, Itti E, Haioun C, Rahmouni A. Whole body MRI and PET/CT in haematological malignancies. *Cancer Imaging* 2007; 7:588–93.
- Schaefer JF, Schlemmer HP. Total-body MR-imaging in oncology. *Eur Radiol* 2006; 16:2000–2015. [\[CrossRef\]](#)
- Casasnovas RO, Meignan M, Berriolo-Riedinger A, et al. SUVmax reduction improves early prognosis value of interim positron emission tomography scans in diffuse large B-cell lymphoma. *Blood* 2011; 118:37–43. [\[CrossRef\]](#)
- Itti E, Lin C, Dupuis J, et al. Prognostic value of interim 18F-FDG PET in patients with diffuse large B-Cell lymphoma: SUV-based assessment at 4 cycles of chemotherapy. *J Nucl Med* 2009; 50:527–533. [\[CrossRef\]](#)
- MacManus MP, Seymour JF, Hicks RJ. Overview of early response assessment in lymphoma with FDG-PET. *Cancer Imaging* 2007; 7:10–18. [\[CrossRef\]](#)
- Safar V, Dupuis J, Itti E, et al. Interim [18F]fluorodeoxyglucose positron emission tomography scan in diffuse large B-cell lymphoma treated with anthracycline-based chemotherapy plus rituximab. *J Clin Oncol* 2012; 30:184–190. [\[CrossRef\]](#)
- Mikhaeel NG. Interim fluorodeoxyglucose positron emission tomography for early response assessment in diffuse large B cell lymphoma: where are we now? *Leuk Lymphoma* 2009; 50:1931–1936.
- Cashen AF, Dehdashti F, Luo J, Homb A, Siegel BA, Bartlett NL. 18F-FDG PET/CT for early response assessment in diffuse large B-cell lymphoma: poor predictive value of international harmonization project interpretation. *J Nucl Med* 2011; 52:386–392. [\[CrossRef\]](#)
- Gu J, Chan T, Zhang J, Leung AY, Kwong YL, Khong PL. Whole-body diffusion-weighted imaging: the added value to whole-body MRI at initial diagnosis of lymphoma. *AJR Am J Roentgenol* 2011; 197:W384–391.
- Abdulqadr G, Molin D, Astrom G, et al. Whole-body diffusion-weighted imaging compared with FDG-PET/CT in staging of lymphoma patients. *Acta Radiol* 2011; 52:173–180. [\[CrossRef\]](#)
- Horger M, Claussen C, Kramer U, Fenchel M, Lichy M, Kaufmann S. Very early indicators of response to systemic therapy in lymphoma patients based on alterations in water diffusivity—a preliminary experience in 20 patients undergoing whole-body diffusion-weighted imaging. *Eur J Radiol* 2014; 83:1655–1664. [\[CrossRef\]](#)
- Tsuji K, Kishi S, Tsuchida T, et al. Evaluation of staging and early response to chemotherapy with whole-body diffusion-weighted MRI in malignant lymphoma patients: A comparison with FDG-PET/CT. *J Magn Reson Imaging* 2015; 41:1601–1607. [\[CrossRef\]](#)
- Mayerhoefer ME, Karanikas G, Kletter K, et al. evaluation of diffusion-weighted magnetic resonance imaging for follow-up and treatment response assessment of lymphoma: results of an 18F-FDG-PET/CT-controlled prospective study in 64 patients. *Clin Cancer Res* 2015; 21:2506–2513. [\[CrossRef\]](#)
- Jensen JH, Helpert JA, Ramani A, Lu H, Kaczynski K. Diffusional kurtosis imaging: the quantification of non-gaussian water diffusion by means of magnetic resonance imaging. *Magn Res Med* 2005; 53:1432–1440. [\[CrossRef\]](#)
- Lu H, Jensen JH, Ramani A, Helpert JA. Three-dimensional characterization of non-gaussian water diffusion in humans using diffusion kurtosis imaging. *NMR Biomed* 2006; 19:236–247. [\[CrossRef\]](#)
- Jensen JH, Helpert JA. MRI quantification of non-Gaussian water diffusion by kurtosis analysis. *NMR Biomed* 2010; 23:698–710. [\[CrossRef\]](#)
- Helpert JA, Adisetiyo V, Falangola MF, et al. Preliminary evidence of altered gray and white matter microstructural development in the frontal lobe of adolescents with attention-deficit hyperactivity disorder: a diffusional kurtosis imaging study. *J Magn Reson Imaging* 2011; 33:17–23. [\[CrossRef\]](#)
- Van Cauter S, Veraart J, Sijbers J, et al. Gliomas: diffusion kurtosis MR imaging in grading. *Radiology* 2012; 263:492–501. [\[CrossRef\]](#)
- Jansen JF, Stambuk HE, Koutcher JA, Shukla-Dave A. Non-gaussian analysis of diffusion-weighted MR imaging in head and neck squamous cell carcinoma: A feasibility study. *AJNR Am J Neuroradiol* 2010; 31:741–748. [\[CrossRef\]](#)
- Suo S, Chen X, Ji X, et al. Investigation of the non-Gaussian water diffusion properties in bladder cancer using diffusion kurtosis imaging: a preliminary study. *J Comput Assist Tomogr* 2015; 39:281–285. [\[CrossRef\]](#)
- Tamura C, Shinmoto H, Soga S, et al. Diffusion kurtosis imaging study of prostate cancer: preliminary findings. *J Magn Reson Imaging* 2014; 40:723–729. [\[CrossRef\]](#)
- Rosenkrantz AB, Sigmund EE, Winnick A, et al. Assessment of hepatocellular carcinoma using apparent diffusion coefficient and diffusion kurtosis indices: preliminary experience in fresh liver explants. *Magn Reson Imaging* 2012; 30:1534–1540. [\[CrossRef\]](#)
- Nogueira L, Brandao S, Matos E, et al. Application of the diffusion kurtosis model for the study of breast lesions. *Eur Radiol* 2014; 24:1197–1203. [\[CrossRef\]](#)
- Suo S, Chen X, Wu L, et al. Non-Gaussian water diffusion kurtosis imaging of prostate cancer. *Magn Reson Imaging* 2014; 32:421–427. [\[CrossRef\]](#)
- Cheson BD, Pfistner B, Juweid ME, et al. Revised response criteria for malignant lymphoma. *J Clin Oncol* 2007; 25:579–586. [\[CrossRef\]](#)
- Pang H, Ren Y, Dang X, et al. Diffusional kurtosis imaging for differentiating between high-grade glioma and primary central nervous system lymphoma. *J Magn Reson Imaging* 2016; 44:30–40. [\[CrossRef\]](#)
- Lin C, Itti E, Luciani A, et al. Whole-body diffusion-weighted imaging with apparent diffusion coefficient mapping for treatment response assessment in patients with diffuse large B-cell lymphoma: pilot study. *Invest Radiol* 2011; 46:341–349. [\[CrossRef\]](#)
- Wu X, Kellokumpu-Lehtinen PL, Pertovaara H, et al. Diffusion-weighted MRI in early chemotherapy response evaluation of patients with diffuse large B-cell lymphoma—a pilot study: comparison with 2-deoxy-2-fluoro-D-glucose-positron emission tomography/computed tomography. *NMR Biomed* 2011; 24:1181–1190. [\[CrossRef\]](#)
- De Paepe K, Bevernaghe C, De Keyser F, et al. Whole-body diffusion-weighted magnetic resonance imaging at 3 Tesla for early assessment of treatment response in non-Hodgkin lymphoma: a pilot study. *Cancer Imaging* 2013; 13:53–62. [\[CrossRef\]](#)
- Grinberg F, Farrher E, Ciobanu L, Geffroy F, Le Bihan D, Shah NJ. Non-Gaussian diffusion imaging for enhanced contrast of brain tissue affected by ischemic stroke. *PLoS One* 2014; 9:e89225.
- Le Bihan D. Apparent diffusion coefficient and beyond: what diffusion MR imaging can tell us about tissue structure. *Radiology* 2013; 268:318–322. [\[CrossRef\]](#)